



**HAL**  
open science

## Green regional aircraft gust response

Sylvie Dequand, Cedric Liauzun

► **To cite this version:**

Sylvie Dequand, Cedric Liauzun. Green regional aircraft gust response. Greener Aviation 2016, Oct 2016, BRUXELLES, Belgium. hal-01400285

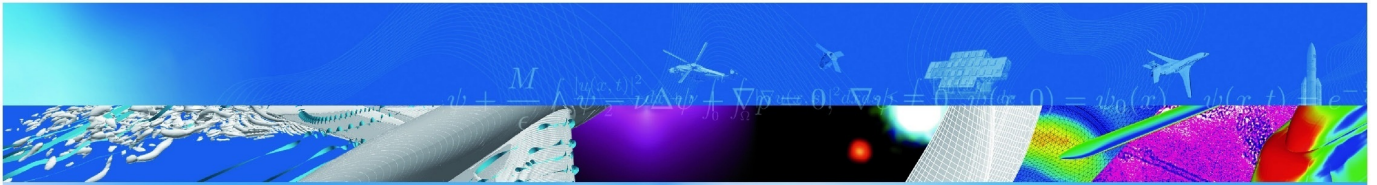
**HAL Id: hal-01400285**

**<https://hal.science/hal-01400285>**

Submitted on 21 Nov 2016

**HAL** is a multi-disciplinary open access archive for the deposit and dissemination of scientific research documents, whether they are published or not. The documents may come from teaching and research institutions in France or abroad, or from public or private research centers.

L'archive ouverte pluridisciplinaire **HAL**, est destinée au dépôt et à la diffusion de documents scientifiques de niveau recherche, publiés ou non, émanant des établissements d'enseignement et de recherche français ou étrangers, des laboratoires publics ou privés.



COMMUNICATION A CONGRES

## **Green regional aircraft gust response**

S. Dequand, C. Liauzun

Greener Aviation 2016  
BRUXELLES, BELGIQUE  
11-13 octobre 2016

TP 2016-684

**70** 2016  
ans

**ONERA**

THE FRENCH AEROSPACE LAB



# GREEN REGIONAL AIRCRAFT GUST RESPONSE

Dequand S.<sup>(1)</sup>, Liauzun C.<sup>(2)</sup>

<sup>(1)</sup> ONERA, The French Aerospace Lab, BP 72, 29 avenue de la Division Leclerc, 92322 CHATILLON Cedex, France, [Sylvie.Dequand@onera.fr](mailto:Sylvie.Dequand@onera.fr) – [www.onera.fr](http://www.onera.fr)

<sup>(2)</sup> ONERA, The French Aerospace Lab, BP 72, 29 avenue de la Division Leclerc, 92322 CHATILLON Cedex, France, [Cedric.Liauzun@onera.fr](mailto:Cedric.Liauzun@onera.fr) – [www.onera.fr](http://www.onera.fr)

**KEYWORDS:** aeroelasticity, fluid-structure coupling simulations, gust load alleviation, load control.

**ABSTRACT:**

This contribution deals with gust load alleviation due to control surfaces deflection time laws. In the framework of the JTI-GRA European project (Green Regional Aircraft), high-fidelity fluid-structure coupling numerical simulations have been performed in order to predict the GTF NLF aircraft gust response (Gear Turbo Fan - Non Laminar Flow).

The ZFW (Zero Fuel Weight) configuration of the GTF aircraft at Mach 0.48 and sea level has been handled and two one peak (1-cos) gusts have been considered. Control laws of the control surface have been provided by Alenia.

Significant load alleviation has been observed for both gust wavelengths when applying the aileron deflection laws.

**1. INTRODUCTION**

Dynamic fluid-structure coupling simulations have been performed using the high fidelity software *elsA* and its aeroelastic module *Ael* in order to assess the gust LC&A (Load Control & Alleviation) devices performances of the GTF-NLF (Gear Turbo Fan - Non Laminar Flow) aircraft [1]. The wing is equipped with an aileron which has been used to alleviate gust loads. “1-cos” single peak gusts, as defined in the certification documents [1], have been considered. Computations have been carried out for the ZFW (Zero Fuel Weight) mass configuration. Control laws have been provided by Alenia and result from a design process using low fidelity aerodynamic models [3] for a Mach number of 0.48 at sea level. Two deflection laws have been provided for the ZFW configuration: one for a gust called “tuned gust” whose frequency of 3.41Hz is close to the aircraft 1<sup>st</sup> eigen mode, and the second law for a gust called “Gust 25 chords”

whose frequency is 1.74Hz. This paper presents the computations of the response to these two gusts using high fidelity numerical simulations.

The first part gives a brief description of the numerical methodology. The structural model, the gust characteristics and deflection laws of the control surface are specified in the second part. The third part is devoted to the analysis of the results of the numerical simulations.

**2. NUMERICAL METHODOLOGY**

**2.1. CFD code *elsA***

Fluid-structure coupling computations are available in the CFD code *elsA* [4], using its optional “*Ael*” subsystem.

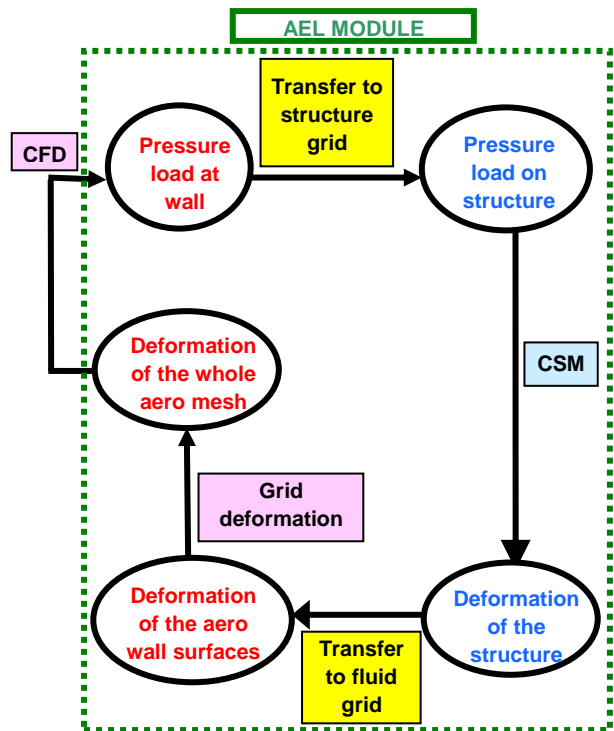


Figure 1: Schematic overview of the methodology used in the *Ael* module of *elsA*

Figure 1 shows a schematic overview of the methodology used in the optional “Ael” module of elsA. The fluid-structure coupling methodology consists in solving the fluid and structure equations in a staggered way within a coupling loop, and in exchanging information at the common fluid-structure interface. The structure solver implemented in elsA-Ael is able to handle models built according to a modal approach or resulting from a condensation of the inverse of the finite element stiffness matrix (flexibility matrix). But only the modal approach can be used for dynamic simulations.

## 2.2. Gust models

The aeroelastic capabilities in elsA-Ael have been developed using an Arbitrary Lagrangian Eulerian formulation (ALE) of the fluid equations. The gust velocity depending on both space and time, has then been introduced as an additional grid deformation speed according to the Sitaraman field velocity approach [5].

Three models of discrete gust are available in elsA: the “sharped edge gust”, the “one minus cosine” often used for certification, and “sine” which could be used for the simulation of harmonic gust response (Figure 2).

The coupling scheme involving the five operations represented in Figure 1 had been introduced within a time consistent scheme in order to be able to perform dynamic coupling simulations. Figure 3 shows an overview of the dynamic coupling scheme, that has been implemented in elsA. This scheme includes an external iteration loop driving the advance in the physical time. A second loop called “coupling loop” is aiming at getting a converged state of both the structure and the fluid within a physical time step.

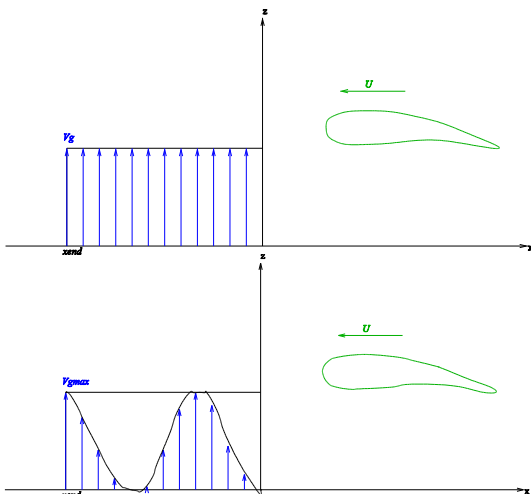


Figure 2: Sharp edge (left) and one minus cosine (right) gust model implemented in elsA.

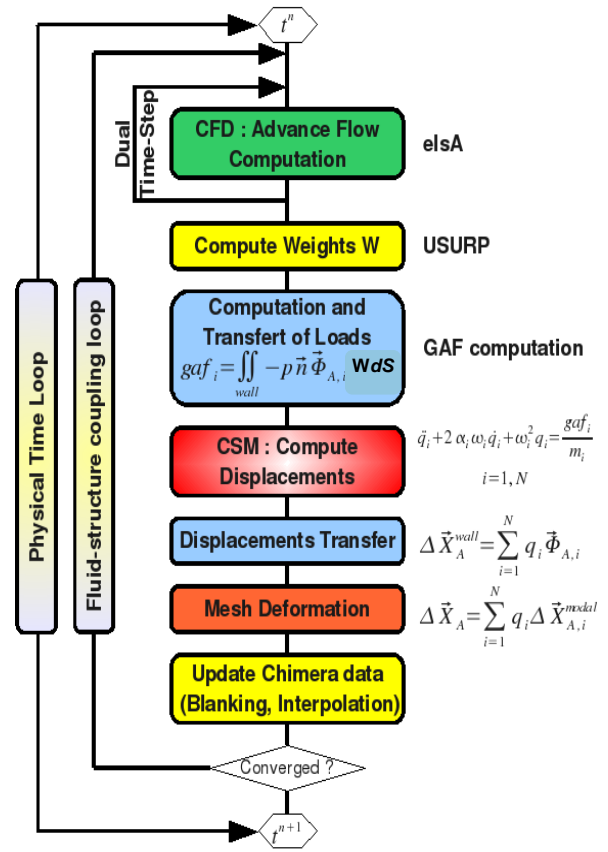


Figure 3: Dynamic modal coupling diagram

The five coupling operations are at last performed within this second loop: flow resolution, transfer from fluid to structure, structure resolution, transfer from structure to fluid, and aerodynamic mesh updating. The flow field is computed using a second order implicit dual time stepping algorithm allowing thus large physical time steps, and the structure displacement using a Newmark one. Furthermore, since dynamic aeroelasticity implies mostly low frequency phenomena and small enough amplitude vibrations so that the structure behavior remains linear, the structure is modelled using a modal approach, which simplifies the fluid-structure transfers and mesh updating operations. The first  $N$  structural modes ( $\vec{\Phi}_s$ ) are indeed mapped to the aerodynamic surfaces ( $\vec{\Phi}_{s,i} \Rightarrow \vec{\Phi}_{A,i}$ ), and  $N$  deformed aerodynamic grids are computed before starting the time iterations ( $(\Delta \vec{X}_{A,i}^{modal})_{i=1,N}$ ). The generalized aerodynamic forces that applies to the structure are deduced straight from the pressure distribution:

$$gaf_i = \iint_{Wall} -p \vec{n} \vec{\Phi}_{A,i} dS . \quad \text{The generalized}$$

coordinates of the structure  $((q_i^n)_{i=1,N})$  are then computed by solving the structure modal equation. And the updated aerodynamic mesh is deduced from them by a simple linear combination of the “modal” aerodynamic meshes:

$$\Delta X_A^n = \sum_{i=1}^N q_i^n \Delta X_{A,i}^{modal} .$$

The yellow boxes in Figure 3 have been added in order to be able to handle overlapping meshes using Chimera techniques.

### 3. MODEL DESCRIPTION

#### 3.1. GTF-NLF configuration

The structural model used is the aeroelastic model of the wing box relevant to the Geared Turbofan (GTF) A/C [1].

The flexible wing box is delimited by the front and rear spars and by the upper and lower skins; it is fitted with 21 ribs, leading edge and LC&A devices (Figure 4). The leading edge is defined by means of lumped masses attached by Nastran rigid body RBE3 elements along the front spar; it has been fitted to the wing box model only to take account of its weight for dynamic and aeroelastic effects.

LC&A devices have been added on the wing box model to be taken into account by aeroelastic computations. The wing is thus equipped with 3 flaps, 2 ailerons (Figure 4) and a winglet. The total weight of the wing model (empty fuel) fitted with leading edge, winglet, LC&A devices and non-structural mass is 2423 kg.

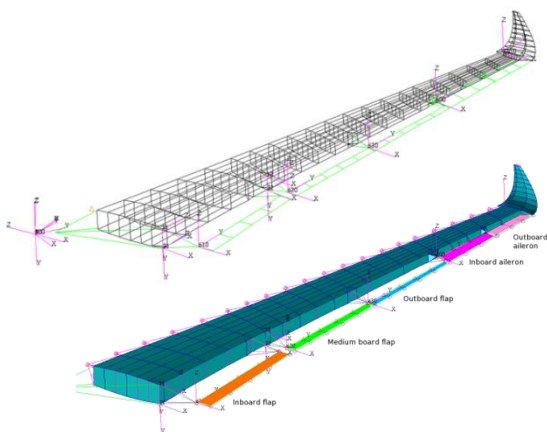


Figure 4: GTF wing box finite element model

#### 3.2. Gust characteristics and control laws

The gust corresponds to a “one minus cosine” single peak vertical gust whose speed  $U$  is defined

with respect to space and time, according to the certification documents [1], as  $U(x, t) = 0.5 \times U_{ds} [1 - \cos(2\pi(x - V_{prop} t)/\lambda)]$  where  $U_{ds}$  is the gust amplitude,  $\lambda$  is the gust wavelength and  $V_{prop}$  the wave propagation speed (equal here to the flight speed).

Control laws for the aileron deflection angle have been determined by Alenia from a design process using low fidelity aerodynamic models [3] for a Mach number of 0.48 at sea level. Two deflection laws have been provided for the ZFW configuration and correspond respectively to:

- a gust called “tuned” gust such that its frequency of 3.41Hz is close to the first eigen mode (3.92 Hz), its amplitude is  $U_{ds}=12.33 \text{ m/s}$ , and its wavelength is  $\lambda=47.93 \text{ m}=12.75 \text{ chord}$ ,
- a gust called “25-chords” gust whose frequency amplitude and wavelength are respectively 1.74Hz,  $U_{ds}=14.36 \text{ m/s}$ , and  $\lambda=93.92 \text{ m}=25 \text{ chord}$ .

Moreover, the initial instant of the time function of the gust speed has been determined to match the initial instant of the aileron deflection law and such that the gust wave reaches the fuselage nose at the instant  $t=0.1 \text{ s}$ . Time evolutions of both gusts and the corresponding deflection laws are given in Figure 5.

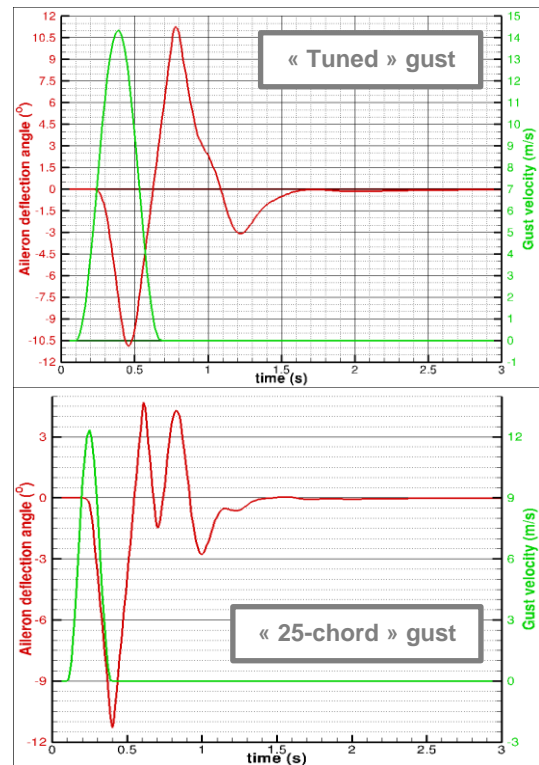


Figure 5: Time evolutions of the vertical gust velocity at the aircraft nose and the corresponding

aileron deflection angle (for the “tuned” and “25-chord” gust).

### 3.3. Numerical simulations

All gust responses have been computed for the aerodynamic conditions matching a flight at Mach number 0.48 and at sea level (zero altitude). Only the ZFW configuration (51356 kg according to the specifications given in [3]) has been studied. This mass configuration matches a lift coefficient of  $C_L=0.555$  (1 g) which is reached with an angle of attack of  $1.4^\circ$ .

Numerical simulations have been performed with a structured mesh made of 78 blocks and about 2.5 million cells. This mesh has been built to model the half fuselage–wing configuration around the initial flight shape of the GTF wing (Figure 6). A static fluid-structure coupling simulation has first been carried out to get the flight shape of the wing for the above aerodynamic conditions. All further dynamic simulations will then be initialized with these static results. Five control surfaces are located on the wing, but the study has been focused on gust load alleviation resulting from the aileron deflection.

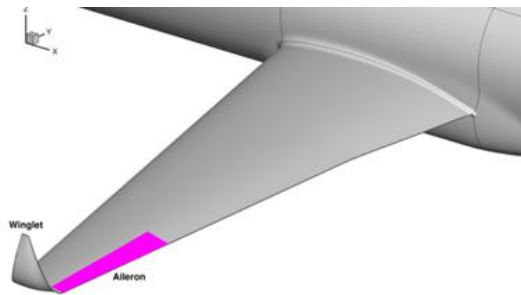


Figure 6: CAD model around the initial flight shape of the GTF-NLF wing. The aileron surface is highlighted in magenta.

Fluid-structure coupling simulations require the building of a reduced order model of the structure. Most of time, dynamic simulations are carried out using a modal representation of the structure. A first step has thus consisted in computing the first eigen modes from the finite element model of the Geared Turbofan (GTF) A/C wing box [1] (Figure 4). Based on static coupling results, 7 modes have been selected for having the most significant contribution to the structure behavior (Figure 7): the first three bending modes, the first two torsion modes and 2 composite ones (mode number 1, 3, 5, 6, 7, 9, 10). Those modes have been obtained by applying clamping conditions in the symmetry plane in order to remove rigid modes. Those 7 modes, which have been computed from the finite element model, have been transferred to the

aerodynamic mesh surfaces of the wing and fuselage using a fitting algorithm based on RBF [6, 7]. The further fluid-structure coupling simulations are performed by neglecting the structural damping.

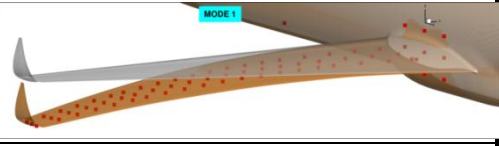
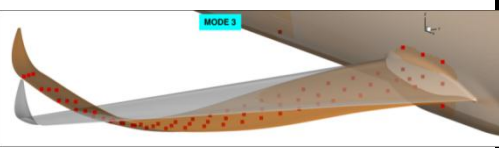
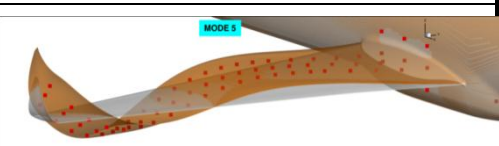
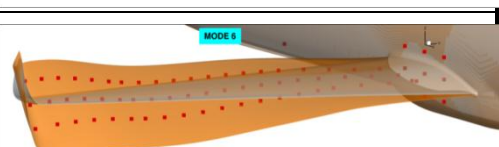
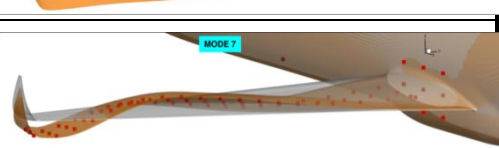
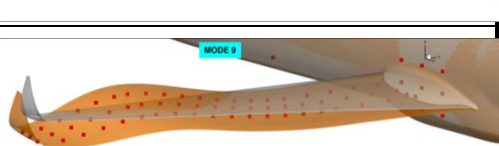
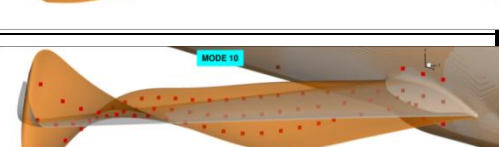
Frequency (Hz)	description	shape
3.92 (Mode 1)	1 <sup>st</sup> bending	
13.05 (Mode 3)	2 <sup>nd</sup> bending	
25.73 (Mode 5)	3 <sup>rd</sup> bending	
28.52 (Mode 6)	1 <sup>st</sup> torsion	
34.81 (Mode 7)	Composite mode	
39.26 (Mode 9)	Composite mode	
46.21 (Mode 10)	2 <sup>nd</sup> torsion	

Figure 7: Structural modes: visualisation of structural nodes (red square symbols), deformed mesh (orange) and undeformed mesh (grey).

## 4. RESULTS

### 4.1. Aileron deflection effect on aerodynamic coefficients

Time simulations have been performed with and without aileron motion, and for both cases with 64

time steps per gust period. This corresponds to  $\delta t = 0.00458s$  for the “tuned” gust and  $\delta t = 0.00898s$  for the “25-chords” gust. Another simulation has been performed without any gust excitation, taking only into account the aileron motion.

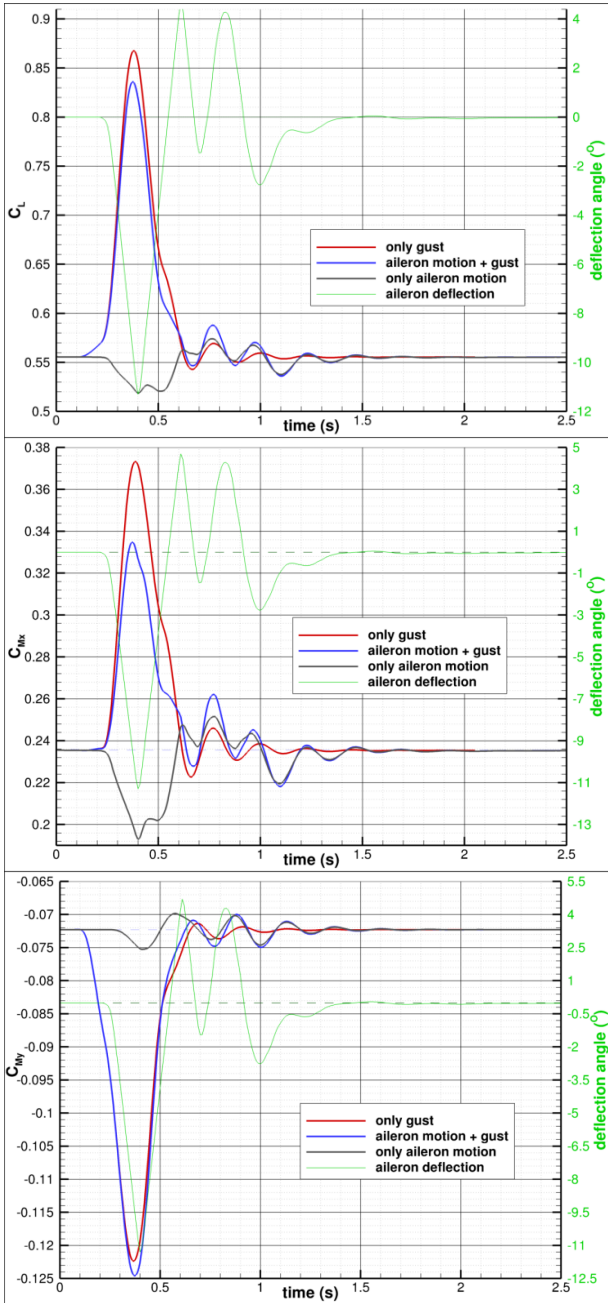


Figure 8: Time evolutions of lift, rolling and pitching moment coefficients response to the “tuned gust” taking (blue curve) and not taking (red) into account the aileron deflection law

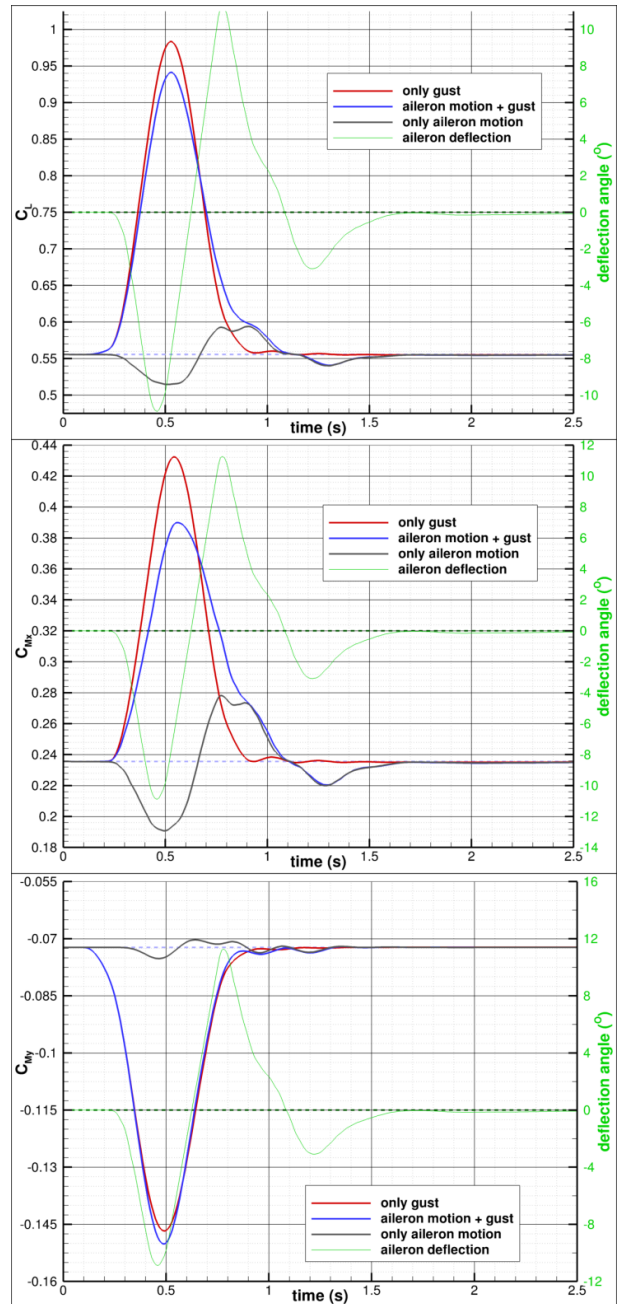


Figure 9: Time evolutions of the aerodynamic coefficients (25 chords gust)

Figure 8 and Figure 9 show the resulting time evolutions of the lift, rolling and pitching moment coefficients for the “tuned” and “25-chords” gust respectively. The aileron motion induces an alleviation of the first peak (peak due to the gust passage) on lift (10.2% and 9.8% for the “tuned” and “25-chords” gust, respectively), and on the rolling moment (28% and 21.5% for the “tuned” and “25-chords” gust, respectively). But a slight



increase of  $-4.5\%$  of the pitching moment is observed for both gusts. In the case of the “25-chords” gust (Figure 9), post gust oscillation of lower amplitude and higher damping than the case of the “tuned” gust is also noticed.

#### 4.2. Aileron deflection effect on generalized coordinates

Figure 10 represents the time evolutions of the 1<sup>st</sup> generalized coordinate (first bending mode) for both gusts.

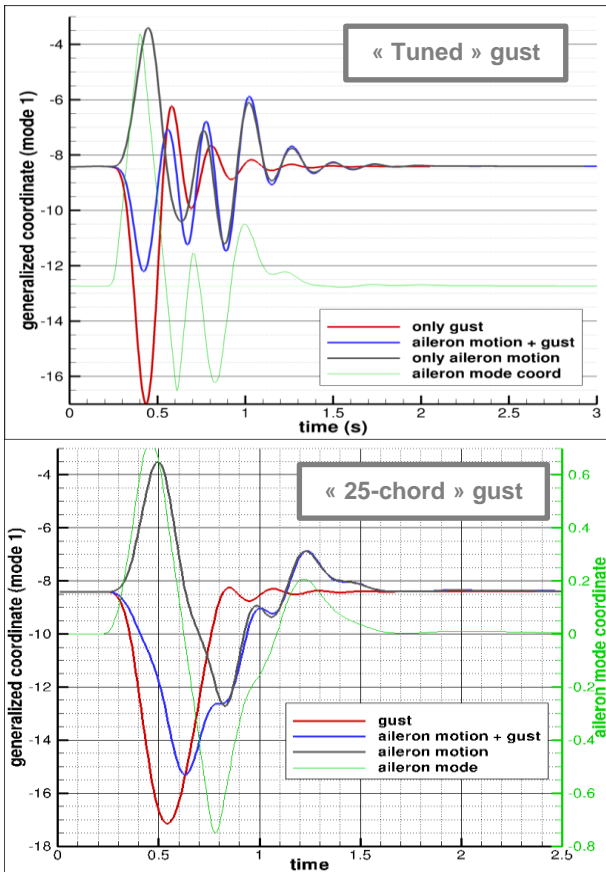


Figure 10: Time evolutions of the 1<sup>st</sup> modal coordinate (1<sup>st</sup> bending) for “tuned” and “25-chords” gust.

The application of the aileron deflection law induces a high decrease of the main peak of the first generalized coordinate (55.8% and 21.8% for the “tuned” and “25-chords” gusts, respectively). This bending mode coordinate shows opposite behaviors when the aircraft is excited by only a gust or by only an aileron motion (red and grey curves in Figure 10: it increases in the gust excitation case while decreasing in the only aileron excitation case. The combination of both excitations tends then to alleviate the main peak.

Especially in the case of the “tuned” gust, the amplitude of the main peak is then getting of the same order as the amplitude of the post gust oscillations. The latter are moreover strongly damped as soon as the aileron stops its deflection motion.

As regards the 4<sup>th</sup> generalized coordinate which matches the first torsion mode (Figure 11), its time behavior is similar to the generalized coordinate of the imposed aileron motion. The pitch moment is indeed increasing with the upward deflection of the aileron. It also increases with the gust passage. The combined excitation of the gust and the aileron motion results then in a peak amplitude almost twice the one resulting from the simulation with only the gust and without any aileron motion (blue and red curves). Nevertheless, only aileron deflection is taken into account and not the horizontal tail plane deflection though the latter may have a strong impact on the moments.

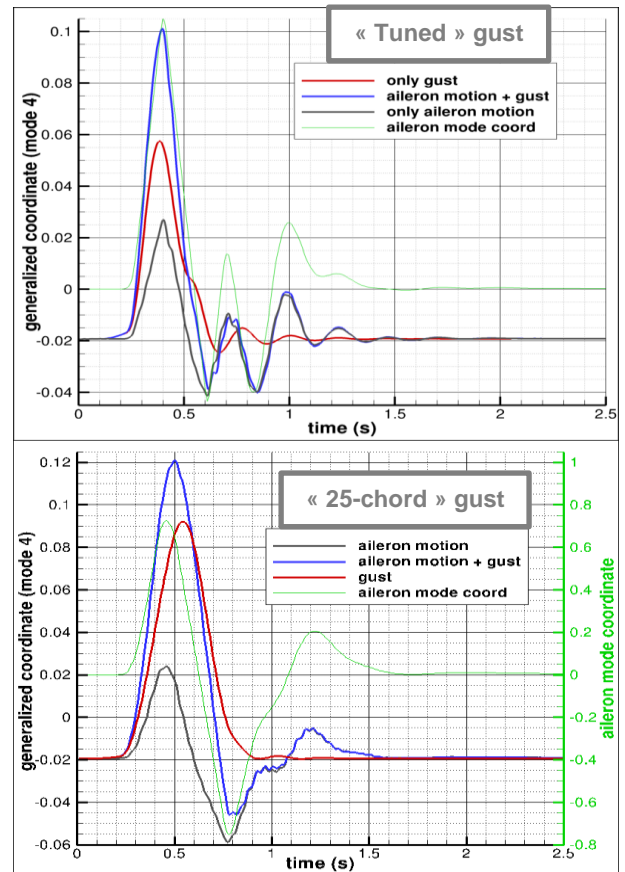


Figure 11: Time evolutions of the 4<sup>th</sup> generalized coordinate (1<sup>st</sup> torsion) for “tuned” and “25 chords” gust.

This 4<sup>th</sup> generalized coordinate seems to be highly sensitive to the aileron motion, and the first upward deflection of the aileron tends to amplify the peak

due to the gust passage. In order to get information from a more physical quantity about the wing deformation, time evolutions of the twist deformation of the wing section close to the wingtip (between the aileron and the winglet root) have been extracted from the simulations. They are very different from the 4<sup>th</sup> generalized coordinates as can be seen in Figure 12 (positive values meaning an increase of the apparent incidence of the section). This shows that the wing twist is highly influenced by other modes than the first torsion one.

Furthermore, a significant alleviation of this twist deformation peak thanks to the aileron motion is noticeable ( Figure 13). Post gust oscillations are indeed in that case of greater amplitude than this first peak.

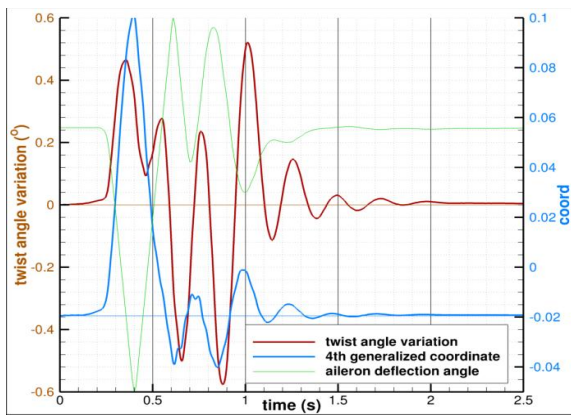


Figure 12: Time evolutions of the twist angle variation of a wingtip section and of the 4<sup>th</sup> generalized coordinate in case of gust with aileron motion (“tuned” gust).

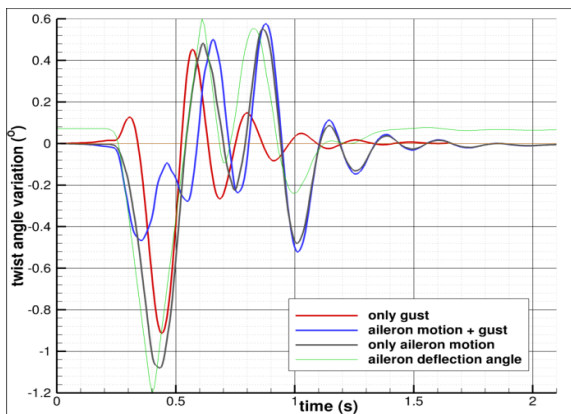


Figure 13: Time evolutions of the twist angle variation of a section close to the wingtip (“tuned” gust).

#### 4.3. Aileron deflection effect on integrated loads

At last, integrated loads have been computed with respect to time for both gust responses (with and

without aileron motion) and for the aileron motion response (without gust) (Figure 14 and Figure 15). In the case of the “tuned” gust (Figure 14), similar time behavior can be noticed for both the shear force and bending moment. The aileron motion induces a significant alleviation of the peak due to the gust passage (11.9% for the shear force and 29.2% for the bending moment). From the torsion moment point of view, the aileron motion induces the peak removal, and resulting secondary oscillations are quickly damped as soon as the aileron motion stops (these oscillations vanish after 2s).

In the case of the “25-chords” gust (Figure 15), a load peak occurs during the gust passage but significant alleviations are obtained when enabling the aileron deflection movement (11.2% on the shear force and 21.6% on the bending moment). Only a slight decrease is observed on the torsion moment (3.7%). Furthermore, post gust oscillations vanish very quickly for this low frequency gust (1.74 Hz whereas the first structural natural frequency is equal to 3.92Hz).

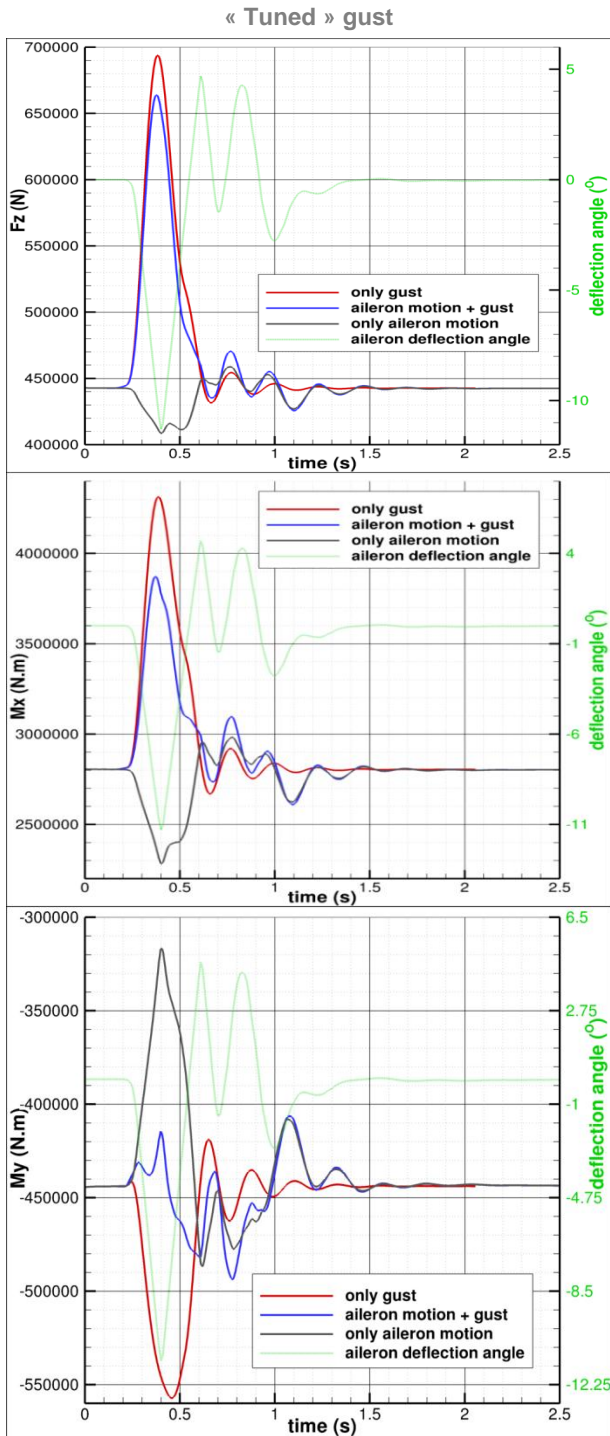


Figure 14: Time evolution of the shear force, the bending and torsion moments at wing root for the "tuned" gust.

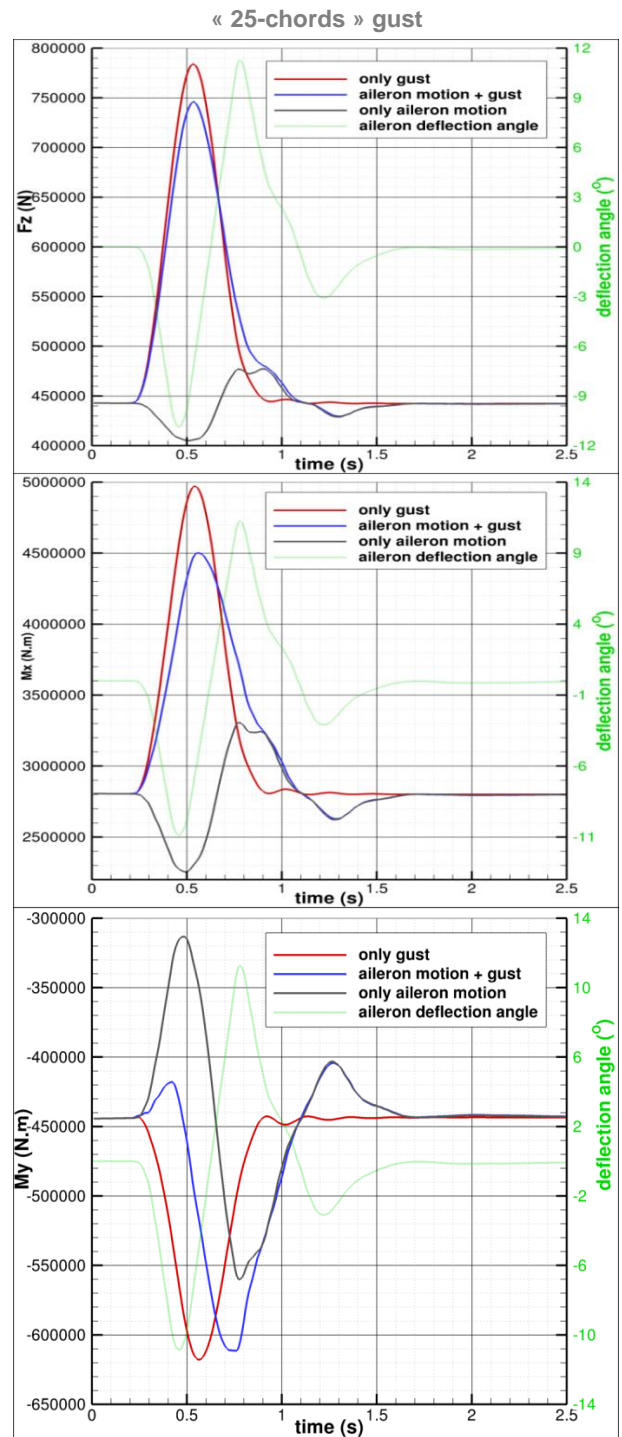


Figure 15: Time evolution of the shear force, the bending and torsion moments at wing root for the "25-chords" gust.

## 5. CONCLUSIONS

Numerical simulations have been performed using high fidelity tools in order to assess gust load alleviation due to control surfaces deflection time law. The ZFW configuration of the GTF aircraft at Mach 0.48 and sea level has been handled and two single peak (1-cos) gusts have been considered: the “tuned” gust whose wave length has been defined to match the first structural natural frequency, and the “25 chords” gust whose wave length is equal to 25 times the mean chord.

Numerical simulations have been performed first with a fixed aileron and second taking into account the time deflection of the aileron, in order to assess the gust load alleviation due to the aileron motion. The structure has been modeled using a modal approach and a reduction to 7 modes which have been selected for being the most contributing to the structure static behavior. Significant alleviations due to the aileron motions have indeed been noticed for both gust excitations and for several load quantities: aerodynamic lift coefficient, aerodynamic rolling moment coefficient, aerodynamic pitching moment coefficient, vertical displacement of the leading edge close to the wingtip, first generalized coordinate matching the 1<sup>st</sup> bending mode of the structure, 4<sup>th</sup> generalized coordinate corresponding to the 1<sup>st</sup> torsion mode, shear force that applies at root, bending moment, and torsion moment (Table 1). Alleviation is of the same order for both gusts for quantities as lift coefficient, rolling moment coefficient, and shear force and bending moment at root, even if alleviation is slightly higher in the case of the tuned gust. But large discrepancies occur for the vertical displacement and the generalized coordinates. Since the first bending mode is one of the most contributing modes to the vertical displacement, resulting alleviation for those two quantities are similar for each gust excitation. But, a significantly higher alleviation has been noticed in the case of the tuned gust. On the other hand different behaviors of the twist and torsion related quantities (4<sup>th</sup> generalized coordinate and torsion moment at root) have been observed. This may be partly explained by the fact that aileron upward deflections aiming at decreasing the lift peak due to gust tends to increase the pitching moment and then the torsion modal coordinate.

Although High fidelity numerical simulations have been performed taking into account only the aileron and neglecting the horizontal tail plane impact, gust load alleviations have been observed, alleviations that are of the same order as these

computed using lower fidelity tools at the control law design stage and presented in [3].

	Tuned gust	25-chord gust
$C_L$	10.2	9.8
$C_{M_x}$	28	21.5
$C_{M_y}$	-4.5	-4.5
Vertical displacement	58	20.7
Modal coordinate 1	55.8	21
Modal coordinate 4	-56.8	26
Shear force at root	11.9	11.2
Bending moment at root	29.2	21.6
Torsion moment at root	-	3.7

Table 1: Load alleviation due to the aileron deflection laws

## 6. ACKNOWLEDGEMENTS

This study was performed in the framework of the JTI-GRA European project. The authors would like to thank Alenia for their contribution.

## 7. REFERENCES

1. GTF A/C Wing Aeroelastic Design Optimised Wing Box – Preliminary Layout. Document N°: GRA-2.1.1-DL(D2.1.1-08)-ALA-TECH-213439 A (2013).
2. EASA CS-25 Subpart C.
3. Calvi N., Baldassin E. (2013). Final assessment of Load Control & Alleviation system for GTF A/C configuration. Document N°: GRA-2.3.1-DL(D2.3.1-05)-ALA-TECH-213488A.
4. Cambier L., Heib S. and Plot S. (2013). The Onera elsA CFD software: input from research and feedback from industry. *Mechanics & Industry*. **14**(03), 159-174.
5. Sitaraman J., Iyengar V. S., Baeder J.D. (2003). On Field Velocity Approach and Geometric Conservation Law for Unsteady Flow Simulations. *16<sup>th</sup> AIAA Computational Fluid Dynamics Conference, Orlando, FL*.
6. Girodroux-Lavigne Ph, Dugeai A. (2003). Transonic aeroelastic computations using Navier-Stokes equations. International Forum on Aeroelasticity and Structural Dynamics (IFASD), Amsterdam (NL)

7. Dugeai A. (2008). Non linear numerical aeroelasticity with the Onera elsA solver. NATO-AVT 152 Limit-Cycle Oscillations and Other Amplitude-Limited, Self-Excited Vibrations, Loen (Norway)



